Precipitation Formation Processes in Convective and Stratiform Clouds as Deduced by Coordinated Polarimetric Radar and Aircraft Measurements

Peter Meischner, Martin Hagen and Hartmut Höller
DLR, Institut für Physik der Atmosphäre

Abstract

For two quite different case studies - an upslope situation in the northern Alpine area and a multicell hailstorm - the processes of precipitation formation were analysed by radar Doppler and polarimetric as well as by coordinated aircraft measurements (for the upslope case). In the upslope situation low density pristine dendrites were formed. Subsequent riming of these particles during their fallout resulted in irregular shapes and a tumbling fall behaviour. The hail formation in the thunderstorm studied was connected with recirculations of graupels and raindrops into the main updraft of the storm.

1. Introduction

The intimate coupling of the cloud microphysical processes with the dynamics of clouds and cloud systems being embedded within the mesoscale circulation patterns, is still far from being sufficiently understood. Short or medium range forecasts especially of severe weather events such as intense precipitation, hail, gusts, downbursts or lightning are by no means satisfactory. Orographic influences further complicate the physical processes involved, making forecasts even more difficult.

A better understanding of these cloud processes - essential for improving forecasts and warnings - may be obtained by model case studies and detailed observational case studies both stimulating and verifying the results of each other. For the observational side aircraft measurements provide dynamical as well as detailed cloud physical parameters with high spatial resolutions along the flight path. The advantage of radar measurements is the synoptic view of complete clouds and cloud systems. With advanced methods, as Doppler measurements and polarimetric measurements, dynamical and microphysical developments can be observed and followed simultaneously. Since 1986 an advanced Doppler-polarization radar - especially designed by DLR for cloud physics research - is operationally used by the Institute of Atmospheric Physics. Examples of precipitation formation processes of a convective and a stratiform situation obtained by combined measurements will be presented.

2. Measurements

2.1. Radar

The radar system POLDIRAD has been described in detail elsewhere (Schroth et al. 1988; Meischner, 1989). The Doppler measurements, giving the radial Doppler velocity and the Doppler spectral width, provide us with wind information (Hagen, 1989) and turbulence parameters as the dissipation rate of kinetic energy (Meyer and Jank, 1990).

The polarimetric measurements result in informations on the type of precipitation. Because the particles of different precipitation classes differ in shape, size distribution and fall behaviour (that means mean orientation with respect to the radar beam and in dielectric constant) and because these parameters influence the backscattering of polarized radar radiation in a different way, some particle classification is possible if radiation of different polarizations is used. Some of the polarimetric parameters available by the POLDIRAD system are summarized in the following (Meischner et al., 1991).

- The reflectivity Z, a measure for particle concentration and mean particle size, because Z is proportional to particle diameter D^6. It further is sensitive to the dielectric constant, which differs between water and ice by a factor of about 4.
- The differential reflectivity Z_{DR}, the ratio of the reflectivities Z_H and Z_V for horizontal and vertical polarized radiation, respectively, allows to identify large raindrops or oriented ice particles like needles or plates.
- The combination of Z and Z_{DR} allows to identify hail and especially to distinguish between heavy rain and hail.
- The depolarization ratio LDR for linear polarized radiation measures that part of the backscattered radiation, which has a polarization state perpendicular to the transmitted one. LDR is indicative for wet ice particles, e.g. wet growing hail or melting graupel.
- Further, the difference reflectivity Z_{DP}, the difference of Z_H and Z_V gives information on particles other than raindrops in a rain-ice mixture (Golestani et al., 1989). The main difference between Z_{DR} and Z_{DP} is given by the fact, that particles of a spherical appearence do not contribute to Z_{DP}.

It is the combination of all these radar polarimetric parameters together with the Doppler measurements which allows to follow precipitation formation processes within different cloud systems.

2.2. Aircraft

The aircraft used for the stratiform case study was the King Air from NCAR, equipped with a complete cloud physics instrumentation, standard meteorological instrumentation and the optical array particle probes, a PMS 2D-cloud probe ($25 - 800\mu m$) and the PMS 2D-precipitation probes ($200 - 6400\mu m$). Futher, a foreward scattering probe - a FSSP - was available for cloud droplet measurements.

3. Hailstorm observations

Hail forming processes have been of great interest in experimental and numerical studies of thunderstorms done in recent years. To a large extent these experiments have been motivated by the intent of artificially modifying these processes in order to prevent damage by large hail at the ground. The seeding concepts and the underlying modification hypotheses did turn out to be inadequate for hail prevention in field studies as NHRE (Knight et al., 1979) and Grossversuch IV (Federer et al., 1986). It was concluded that a better understanding of the basic physical processes was crucial for further progress.

A case study of a multicell storm is presented. The storm was observed on June 30, 1990 in Southern Germany. Here we address not only the question of hydrometeor discrimination but also the hydrometeor development in the general framework of storm dynamics. Doppler measurements reveal a general picture of the flow conditions in the hail regions of the storm. Positive values of Z_{DR} above the freezing level in the storm indicate the presence of supercooled drops. Their position relative to typical reflectivity features like the weak echo region or the vault is shown. Thus a more complete picture of thunderstorm processes can be obtained.

The series of volume scans taken during the evolution of the storm clearly showed its multicell structure. A sequence of cells in different stages of their development was detectable throughout the whole evolution of the storm. Some of these cells were just growing and forming graupel particles, the mature ones contained hailstones aloft and the fallout of precipitation occured in the dissipating cells. As an example Fig.1 shows a horizontal section through the storm at 6 km height above ground. A vertical scan constructed from the time series data taken at 328° azimuth about 8 min prior to the horizontal scan is presented in Fig.2.

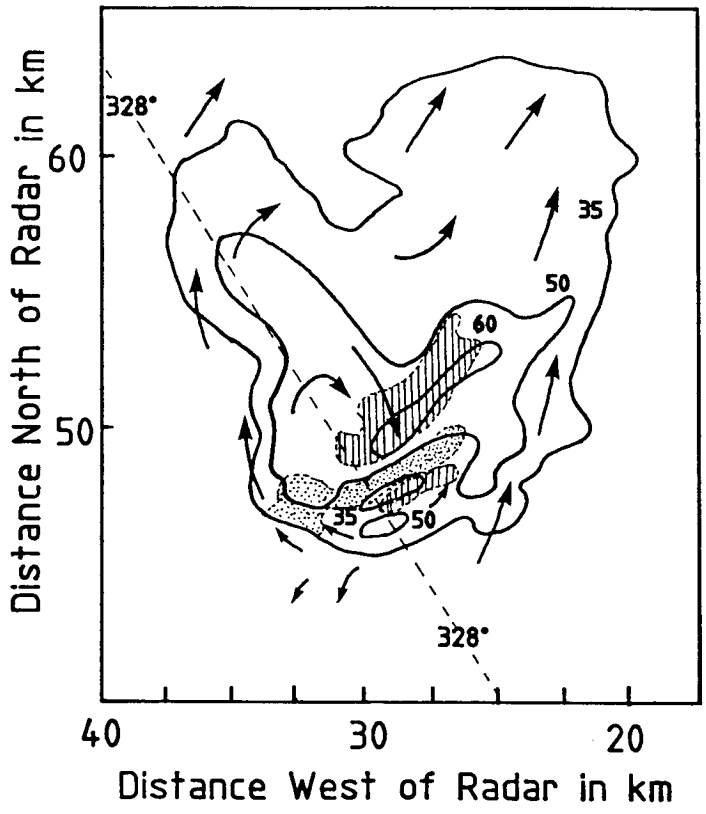

Fig.1: Horizontal section of different radar parameters at 6 km height above ground. The scan was taken at 14:46 UTC and advected to 14:38 UTC with the mean storm motion for comparison with Fig.2. Solid contours: reflectivity Z_{HH} in dBZ. Hatched area: LDR > 10 dB. Dotted area: Z_{DR} > 1 dB at 5 km above ground.

A bounded weak echo (BWER) region at 29 km west and 47 km north of the radar is to be seen very clearly from Fig.1. It is located just south of the main echo core which shows reflectivity values of 63 dBZ and high LDR. The direction of storm propagation is approximately to the east. As the area of positive Z_{DR} at 6 km height is rather small in the section shown in Fig.1 the region of Z_{DR} > 1 dB is indicated for 5 km height. Thereby its position relative to the reflectivity contours is not changed but can be demonstrated more clearly.

The structure of the storm relative flow is indicated by the arrows in Fig.1 and Fig.2 in a qualitative sense. It is derived from the single Doppler measurements. The main

characteristics of the wind field at mid-levels are the anti-cyclonic rotation in the western parts of the main storm core and a divergent flow at the southern edge of the storm in the region of new cell growth. These cells then travelled either around the western storm flank in an anticylonic path or around the eastern flank in a cyclonic path. But the main and most intense hailshaft was mostly present directly beneath the BWER. Velocity components towards the radar were relatively high in the region of high reflectivity and high LDR (Fig.1). According to the vertical cross section (Fig.2) this is the region of the main thunderstorm downdraft.

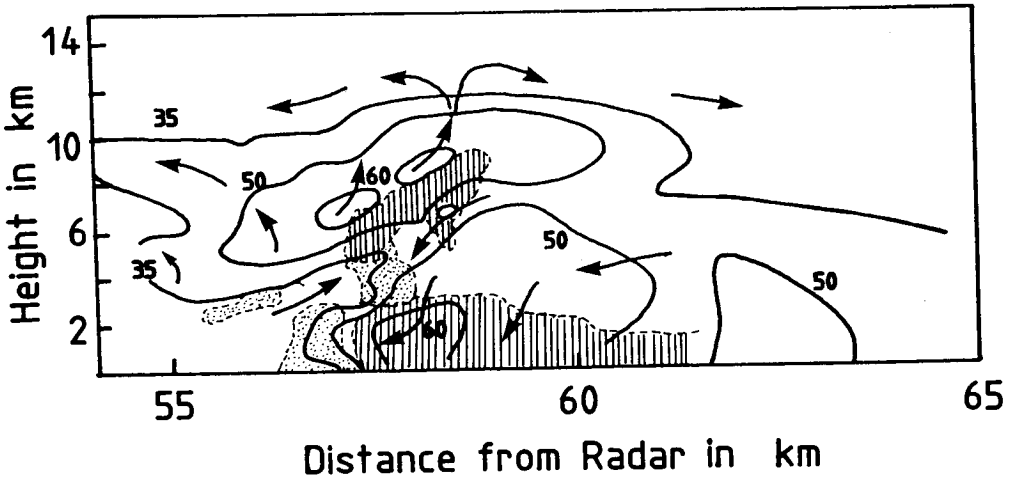

Fig.2: Vertical section of different radar parameters at 328° azimuth (see Fig.1). The scan was taken at 14.38 UTC in time series mode. Solid contours: reflectivity Z_{HH} in dBZ. Hatched area: LDR > 10 dB. Dotted area: Z_{DR} > 1 dB.

From the dynamical flow structure as indicated by the Doppler measurement we are led to conclude, that the positive-Z_{DR} region extending around the main precipitation shaft is located at the intersection of the storm's main updraft and downdraft. Possibly, small melting hailstones, graupel particles or raindrops are recirculated into the updraft following a clockwise trajectory in Fig.2. Such raindrops could thus be carried up into regions well above the freezing level in a supercooled stage. For such a recirculation to occur the updraft speeds have to exceed the terminal fall velocities of the drops (about 10 m s^{-1}), an assumption which seems quite reasonable for the main updraft of the storm.

Another possibility for the formation of raindrops aloft is a counter-clockwise recirculation of graupel particles formed in the forward flank overhang and a subsequent melting as the graupel fall below the melting level (at 55 to 56 km range in Fig.2). The overhang structure is connected with the new cells growing on the southern periphery of the storm. These particles first fall against the updraft, but, as the updraft speed increases towards the inner parts of the storm, the drops may begin to rise again, not falling out prematurely to the ground.

The main formation region for the hailstones can be seen between 6 and 8 km height in Fig.2. Increased LDR values are found in the areas close to the weak echo region indicating wet growth of ice particles.

4. Stratiform precipitation

At the initiation of stratiform precipitation a variety of different ice particles may be involved. In order to study this process some knowledge on the kind of particles and their size distribution is required. Aircraft measurements allow for an identification of hydrometeor types. However, the measurements are confined to small parts of the cloud system which are penetrated by the aircraft. On the other hand, radar measurements allow for a rapid overview of a more complete precipitation system within some minutes. Particle identification by radar measurements is possible only by a combination of different polarimetric radar parameters. For identifying small ice particles such as needles, stellar dendrites, plates or aggregates a most successful strategy is to analyse the particle distributions by in situ methods simultaneously with radar observations. Furtheron, model calcluations of the electromagnetic backscatter for the different particles substantiate the interpretation of radar measurements.

Coordinated measurements were performed in November and December 1987 with POLDIRAD and the King Air aircraft of NCAR in the Alpine foreland south to Oberpfaffenhofen.

4.1. Weather situation

On 27 November 1987, an upslope situation developed at the northern Alpine area caused by a low pressure system to the south of the Alps. Moist mediterranian air was forced around the east of the Alps and the low level winds from the north maintained the upslope conditions during the observation period. First layer clouds initially formed southwest of Oberpfaffenhofen. During the forenoon the system developed to form widespread snowfall. The Radar measurements (Fig.3) show increasing precipitation rates towards the Alps.

4.2. Measurements

PPI and RHI scans of polarimetric, reflectivity as well as Doppler data were taken frequently to record the temporal and spatial evolution of the precipitation system. Fig.3 shows the reflectivity (Z_{HH}), differential reflectivity (Z_{DR}) and reflectivity difference (Z_{DP}) for a RHI scan at 210° azimuth. At a range of 32.5 km and an altitude of 2.4 km the radar echo of the King Air aircraft can be located. The reflectivity (Z_{HH} and Z_{VV}, HH and VV indicates horizontal or vertical polarization, respectively; the first stands for transmit and the second for receive) is mainly dominated by the size of the particles and less by the number concentration of the particle size distribution.

In Fig.3 the reflectivity shows low values close to the radar and high values close to the mountains (range greater 30 km). This indicates that particle sizes increase towards the Alps. For the close ranges at higher altitudes the Z_{DR} signal indicates particles with preferred horizontal orientation, whereas close to the mountains and at low altitudes particles of sphercial appearance, irregular in shape or tumbling are recorded. Z_{DP} indicates that in the region with high Z_{DR} (> 4 dB) only particles of low concentration can be present, because Z_{HH} and Z_{VV} both must be small to result in a large ratio but small difference.

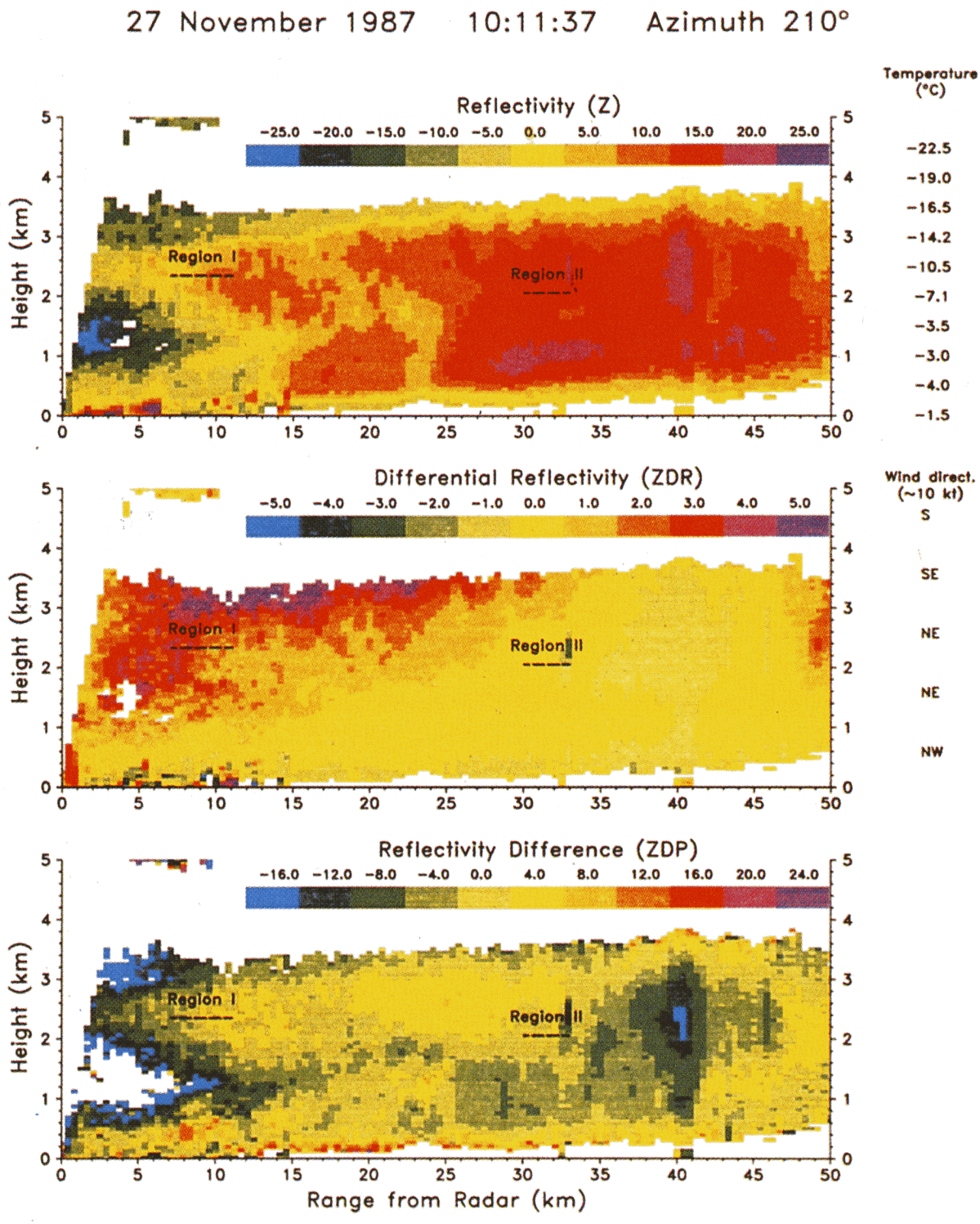

Fig.3: Radar scan at 10:11 UTC, Nov. 27, 1987. Azimuth angle 210°. The comparison with King Air data was made in region I and II.

For the comparison with the aircraft measurements two regions along the flight track of the King Air were selected. Region I is with low Z_{HH}, high Z_{DR} and low Z_{DP}. Here dendrites, plates or needles are expected. In region II Z_{HH} is high, Z_{DR} and Z_{DP} are about zero, here aggregates are expected. Fig.4 shows scatterplots of the radar parameters for these two regions. The points are the data from the individual radar sample volumes within a 400 m deep box within the marked areas. The scattergrams show clustering of the data points in different regions. It is assumed that the position of the data points within the cluster is given by the prevailing particle size distribution within the sample volume. The dashed line in the Z_{HH} - Z_{DP} scattergram is termed as "rain line", because, according to electromagnetic scattering computations and observations, radar measurements in rain should lie on this line.

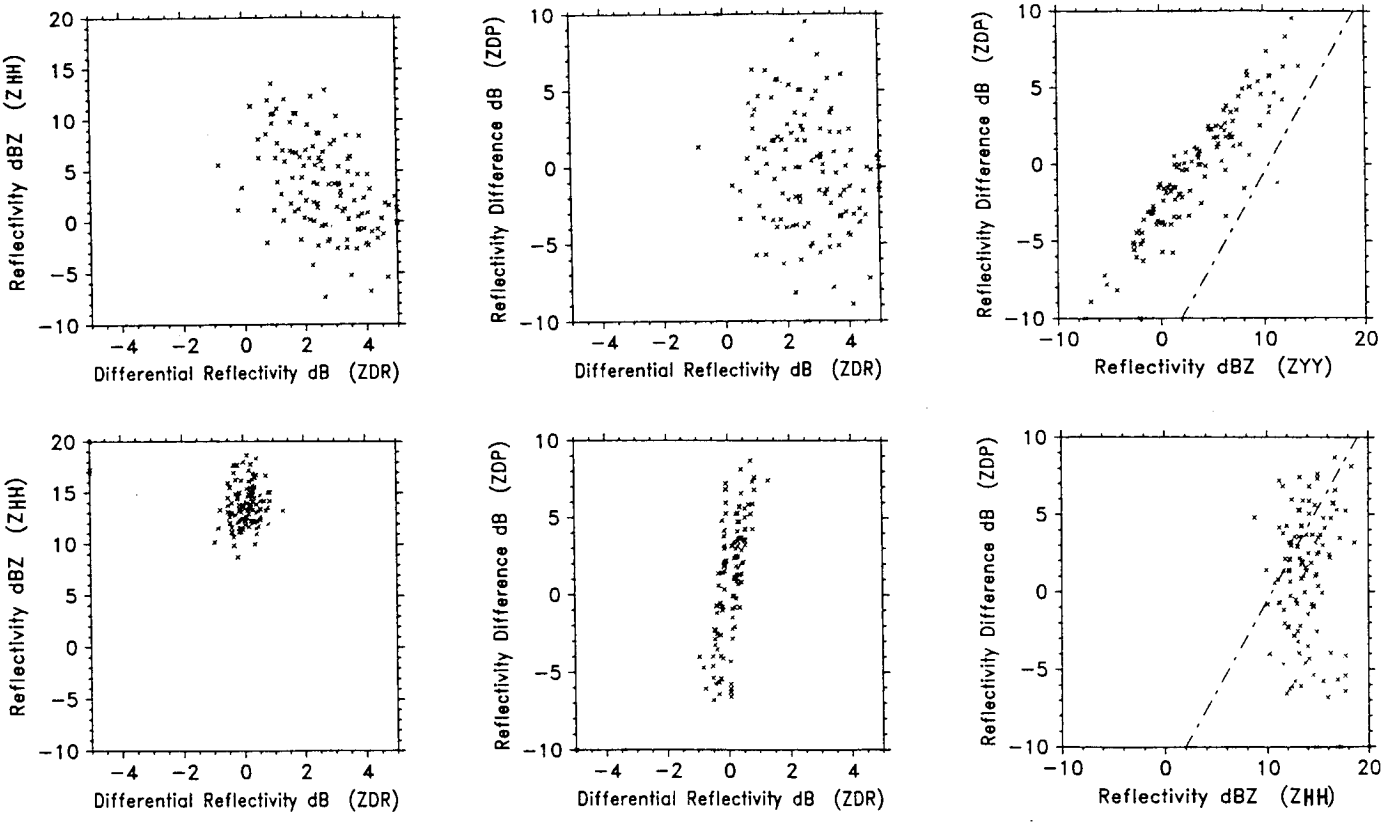

Fig.4: Scattergrams of radar parameters Z_{HH}, Z_{DR} and Z_{DP}. Top row: scattergrams for data points around region I; bottom row: same for region II.

The flight tracks of the King Air were along the 210° radial with respect to the radar at four different altitudes (3050 m MSL, 2650 m MSL, 2350 m MSL, and 2050 m MSL). Maximum distance from the radar was 35 km.

One goal of this project was to intercompare the polarimetric radar measurements with simultaneous in situ measurements of the particle populations. The strategies for particle classification from the PMS probes measurements therefore were guided not only by cloud physical considerations but also by aspects connected to the electromagnetic scattering behaviour of such particles.

4.3. Results

Particle classification was performed into the following groups:

- Dendrites, hexagonal plates (orientated fall behaviour, low Z_{HH}, high Z_{DR});
- Aggregates (tumbling fall behaviour, medium Z_{HH}, zero Z_{DR});
- Graupel (tumbling fall behaviour, high Z_{HH}, zero Z_{DR});
- Needles (orientated fall behaviour, low Z_{HH}, medium Z_{DR});
- Droplets (orientated fall behaviour, medium Z_{HH}, low Z_{DR}).

Classification of the observed particles was done manually on a particle by particle basis. This procedure is very time consuming, but more reliable than automatic procedures as described e.g. by Duroure (1982). The automatic procedure failed in distinguishing stellar dendrites from aggregates. Fig.5 shows the results of the manual classification for two selected regions (marked as region I and II in Fig.3). The group named "other" consits of unclassificable or irregular particles. In region I dendrites are dominating, whereas in region II aggregates and rimed dendrites are prevailing.

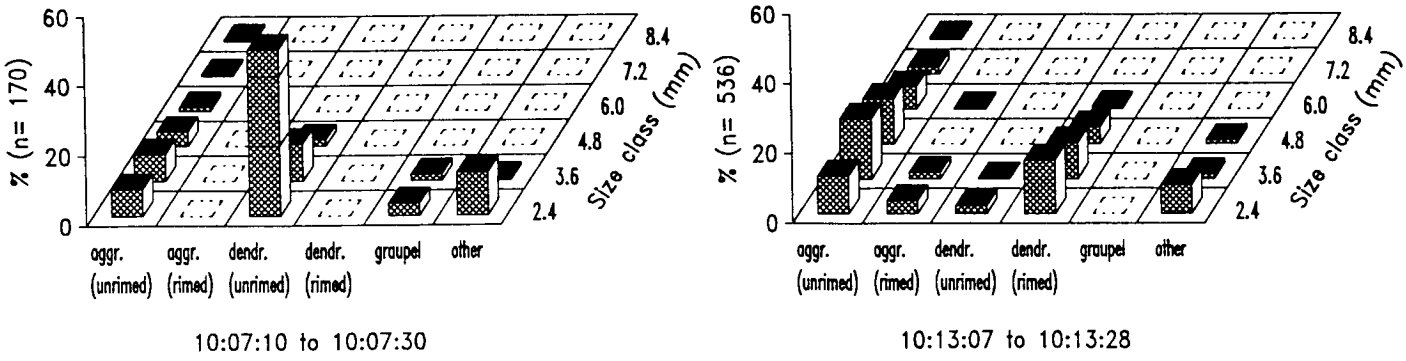

Fig.5: Classification of particles observed by PMS 2D-P probes. Left: Region I; right: region II.

This example shows, that cloud areas dominated by dendrites can clearly be separated from areas dominated by aggregates by using combined and well coordinated radar and aircraft measurements. Radar measurements show the two- or three-dimensional situation in a cloud system. It is assumed that mixtures of dendrites and aggregates as well as transitions between them can be identified by the clustering of radar data points between the clusters as shown in Fig.4. Assuming this, the radar measurements (Fig.3) can be interpreted as follows.

Close to the radar, low density pristine dendrites were formed in altitudes above 3000 m. The temperature there is about -14°C. With decreasing altitude the dendrites begin riming and their fall behaviour and their shape becomes more and more irregular, resulting in a lower Z_{DR}. Further, with increasing particle size and number density the reflectivity also increases. The region between 1000 m and 2000 m above ground is characterized by an inversion combined with a windshift from northwesterly to northern winds. Slightly rising of the air within the inversion would result in a subsaturation. Therefore evaporation of particles takes place, consistent with the observed decrease in reflectivity. Below 1000 m small but irregular particles are left which then fall to the ground. From the observation of increasing reflectivity towards

the ground it might be concluded that the particles are still growing by riming and aggregation.

Because of the steeper slope of the terrain, the updraft is larger close to the Alps, the residence time of the particles (dendrites and aggregates) is increased and therefore growing by coalescence and riming results in an increasing precipitation intensity.

References:

Duroure, C., 1982: Une nouvelle méthode de traitement des images d'hydrométéores données par les sondes bidimensionnelles. J. Rech. Atmos., 6, 71-84.

Federer, B., A. Waldvogel, W. Schmidt, H.H. Schiesser, F. Hampel, M. Schweingruber, W. Stahel, J. Bader, J.F. Mezeix, N. Doras, G. D'Aubigny, G. DerMegreditchian and D. Vento, 1986: Main results of Grossversuch IV. J. Climate Appl. Meteor., 25, 917-957.

Golestani, Y., V. Chandrasekar and V.N. Bringi, 1989: Intercomparison of multiparameter radar measurements. Proc. 24nd Radar Meteor. Conf. Thallahassee, Amer. Meteor. Soc., Boston, 309-314.

Hagen, M., 1989: Ableitung von Windfeldern aus Dopplermessungen eines Radars und Anwendung auf eine Kaltfront mit schmalem Regenband. Dissertation Universität München, DLR Forschungsbericht FB 89-61, 108pp.

Knight, C.A., G.B. Foote and P.W. Summers, 1979: Results of a randomized hail suppression experiment in Northeast Colorado. Part IX: Overall discussion and summary in the context of physical research. J. Appl. Meteor., 18, 1629-1639.

Meischner, P.F., 1989: Observations of dynamical and micropysical aspects related to hail formation with the polarimetric Doppler radar Oberpfaffenhofen. Theor. Appl. Climatol., 40, 209-226.

Meischner, P.F., V.N. Bringi, D. Heimann and H. Höller, 1991: A squall line in Southern Germany: Kinematics and precipitation formation as deduced by advanced polarimetric and Doppler radar measurements. Mon. Wea. Rev., 119, 678-701.

Meyer, W. and T. Jank, 1990: Doppler spectra from incoherent backscatter: Principles and examples of application for POLDIRAD. ESA Technical Translation, ESA-TT-1197, 59p.

Schroth, A.C., M.S. Chandra and P.F. Meischner, 1988: A C-band coherent polarimetric radar for propagation and cloud physics research. J. Atmos. Ocean. Techn., 5, 803-822.